Journal of Power Sources 205 (2012) 100–107

Contents lists available at SciVerse ScienceDirect

Journal of Power Sources

journal homepage: www.elsevier.com/locate/jpowsour

Phase formation and properties of composite electrolyte $BaCe_{0.8}Y_{0.2}O_{3-\delta}$–$Ce_{0.8}Gd_{0.2}O_{1.9}$ for intermediate temperature solid oxide fuel cells

Dong Lin [a], Qunhao Wang [a], Kaiping Peng [a,*], Leon L. Shaw [b,**]

[a] College of Materials Science and Engineering, Fuzhou University, Fuzhou, Fujian, China
[b] Institute of Materials Science, University of Connecticut, Storrs, CT, USA

ARTICLE INFO

Article history:
Received 10 November 2011
Received in revised form
28 December 2011
Accepted 1 January 2012
Available online 9 January 2012

Keywords:
Intermediate temperature solid oxide fuel cells
Composite electrolyte
Electrochemical performance
Phase transformation

ABSTRACT

In this study, we have investigated the feasibility of forming a new ionic conducting electrolyte from a proton conducting phase, $BaCe_{0.8}Y_{0.2}O_{3-\delta}$ (BCY), and an oxygen conducting phase, $Ce_{0.8}Gd_{0.2}O_{1.9}$ (GDC), in order to decrease the reduction of Ce^{4+} ions to Ce^{3+} ions in reducing atmospheres at high temperatures. BCY–GDC composite powders (molar ratio 1:1) are synthesized via a one-step citric acid–nitrate gel combustion method. The reaction between the BCY and GDC in these composite powders at 1550 °C results in the formation of a new perovskite phase with a nominal composition of $BaCe_{1.6}Y_{0.2}Gd_{0.2}O_{4.9-\alpha}$. The conductivity of the new perovskite phase is found to be substantially (~150%) higher than that of the composite electrolyte made from the mixture of BCY and GDC with the same nominal composition as the new perovskite phase. The single fuel cells with the new perovskite electrolyte exhibit better electrochemical performance than the cells with the composite electrolyte made of the mixture of BCY and GDC. The maximum power density of single cells with the new perovskite electrolyte can reach 0.657 W cm^{-2} at 700 °C using humidified hydrogen (3% H_2O) as the fuel. This maximum power density is ~65% higher than that of the cells with the BCY + GDC composite electrolyte.

© 2012 Elsevier B.V. All rights reserved.

1. Introduction

Doped CeO_2-based fluorite cubic materials have attracted extensive attention worldwide lately owing to their potential as the electrolyte for solid oxide fuel cells (SOFCs) to operate at intermediate temperatures [1–8]. Such enormous interest derives from the much higher ionic conductivity of doped ceria electrolytes than the state-of-the-art electrolyte made of yttria-stabilized zirconia (YSZ) [1]. However, Ce^{4+} ions can be thermodynamically reduced to Ce^{3+} ions in reducing atmospheres at high temperatures, causing internal shortening and decrease in open circuit voltage (OCV) and output power density [9–11]. To combat this problem, several approaches have been explored. One of these approaches is to use bilayer electrolytes with a thin film resisting to reduction (such as YSZ) on the fuel side of the doped ceria electrolyte [12,13]. However, it is found that at long operation times interdiffusion takes place, leading to the dissolution of the thin YSZ film into the doped ceria electrolyte [13].

Another approach to address the reduction issue of doped ceria is through the design of composite electrolytes [14–18]. A composite electrolyte of $Ce_{0.8}Sm_{0.2}O_{1.9}$ dispersed in a YSZ matrix reduces the electronic conductivity [14]. SOFCs constructed using the composite electrolyte made of Gd-doped ceria and Gd-doped barium cerate exhibit higher OCVs compared to those based on Gd-doped ceria alone [15]. The electrolytes based on the mixture of a proton conductor ($BaCe_{0.8}Y_{0.2}O_{3-\delta}$) and an oxygen ion conductor samarium doped ceria ($Ce_{0.8}Sm_{0.2}O_{2-\delta}$) [17] or the mixture of $BaCe_{0.8}Sm_{0.2}O_{3-\delta}$ and $Ce_{0.8}Sm_{0.2}O_{2-\delta}$ [18] have all resulted in higher OCVs than those based on Sm-doped ceria alone. The peak power density exhibited by the SOFC with the composite electrolyte made of $BaCe_{0.8}Sm_{0.2}O_{3-\delta}$ and $Ce_{0.8}Sm_{0.2}O_{2-\delta}$ is high (505 mW cm^{-2} at 700 °C), indicating the potential of the composite electrolyte approach [18].

The improved OCV and reduced electronic conductivity of composite electrolytes have been generally attributed to the electron blocking effect of the second phase to the leakage current generated by the reduction of the doped ceria [14–18]. In the case of mixing a proton conductor with doped ceria, the composite electrolyte has an additional advantage of conducting oxygen ions and proton simultaneously if H_2 fuel is used [17]. Better chemical stability of the electrolyte can also be achieved if the composition of the composite electrolyte is properly selected. As in the case of the $BaCe_{0.8}Sm_{0.2}O_{3-\delta}$ plus $Ce_{0.8}Sm_{0.2}O_{2-\delta}$ mixture [18], the $BaCe_{0.8}Sm_{0.2}O_{3-\delta}$ matrix can protect the $Ce_{0.8}Sm_{0.2}O_{2-\delta}$ from reduction, while the $Ce_{0.8}Sm_{0.2}O_{2-\delta}$ matrix can protect $BaCe_{0.8}Sm_{0.2}O_{3-\delta}$ from corrosion caused by CO_2 and H_2O.

* Corresponding author. Tel.: +86 13509398856.
** Corresponding author.
E-mail addresses: pkp715@163.com (K. Peng), leon.shaw@uconn.edu (L.L. Shaw).

0378-7753/$ – see front matter © 2012 Elsevier B.V. All rights reserved.
doi:10.1016/j.jpowsour.2012.01.033

In this study, we have investigated the feasibility of a new approach to form novel ionic conductors with high resistance to the reduction of doped ceria. This is done by reacting a proton conductor, $BaCe_{0.8}Y_{0.2}O_{3-\delta}$ (BCY), with the oxygen ion conductor, $Ce_{0.8}Gd_{0.2}O_{1.9}$ (GDC) to form a new phase. BCY is known to resist reduction at the reducing atmosphere and has been used for the composite electrolyte as mentioned above [17]. As such, the new phase formed from the reaction between BCY and GDC may have the potential to possess better resistance to the reduction by reducing atmospheres than pure GDC. To form the new phase, we have reacted BCY and GDC at 1550 °C at the solid state and compared the total conductivity of the new phase with those of the BCY + GDC composite electrolytes. Furthermore, SOFCs with the new phase as the electrolyte are constructed and evaluated for their performance at intermediate temperatures (450–700 °C). The electrochemical performance of the SOFCs with the new phase electrolyte is also compared with that of the SOFCs with the BCY + GDC composite electrolytes. These comparisons reveal that the new phase derived from the reaction between BCY and GDC is better than the composite electrolytes made of the BCY and GDC mixture in all of the properties and performance that we have evaluated. The details of our findings are reported below.

2. Experimental

2.1. BCY–GDC power synthesis and sintering

$BaCe_{0.8}Y_{0.2}O_{3-\delta}$–$Ce_{0.8}Gd_{0.2}O_{1.9}$ composite electrolyte powders (BCY–GDC with a molar ratio 1:1) were synthesized via a one-step citric acid–nitrate gel combustion method using the procedure described in Ref. [18]. $Ba(NO_3)_2$, $Ce(NO_3)_3{\cdot}6H_2O$, $Y(NO_3)_3{\cdot}6H_2O$ and Gd_2O_3 were used as the starting materials for the synthesis, while ethylenediaminetetraacetic acid (EDTA) and citric acid (CA) were used as chelating agents. The synthesis procedure started with adding an appropriate amount of dilute nitric acid to a mixture of Gd_2O_3, $Ce(NO_3)_3{\cdot}6H_2O$ and $Y(NO_3)_3{\cdot}6H_2O$. Subsequently, the mixture of $Ba(NO_3)_2$, EDTA and CA was dissolved in dilute aqueous ammonia. The concentrations of the CA and EDTA added were such that the molar ratio of the total metal ions in the final solution to CA and EDTA was 1:2:1. The two solutions above were mixed, heated and stirred continuously at about 70 °C until gelling. The pH value of the above solution was adjusted to 7 during stirring using aqueous ammonia. The gel formed was then moved to an evaporation pan heated on a hot plate. Gel ignition and combustion then occurred, giving the as-prepared powders. The as-prepared powders were then calcined at 1000 °C for 5 h.

For sintering and phase formation studies, the BCY–GDC composite electrolyte powder was pressed into discs with a diameter of 12 mm and a thickness of 0.5 mm under a pressure of 300 MPa. The discs were subsequently sintered at 1150 °C, 1250 °C, 1350 °C, 1450 °C or 1550 °C for 5 h in air with a heating rate of 3 °C min^{-1}.

2.2. Characterization of the BCY–GDC electrolyte

Phase structures of the as-prepared powders and the electrolyte discs sintered at different temperatures were identified via X-ray diffraction (XRD) using CuK_α radiation on an UltimaIII type diffractometer. The working voltage is 35 kV with the tube current 20 mA, the scanning range 20–90° and scanning speed 2° min^{-1}. The crystallite size, d, of the calcined powders was estimated using the Scherrer formula [19].

The relative density of the sintered discs was measured via Archimedes principle. The surface microstructures of the discs sintered at different temperatures were investigated using scanning electron microscopy (SEM, S-3000N). For conductivity (σ) measurement, silver paste was painted onto both sides of the sintered discs, and baked at 600 °C for 2 h to burn out organic binder and formed Ag electrodes. The conductivity of the discs was measured in wet air (3% H_2O) from 550 to 800 °C using the two-probe method with the aid of an alternating current impedance analysis apparatus (WAYNE KERR6540A). The frequency ranged from 1000 Hz to 20 MHz. The total conductivity was calculated from the measured resistance, R, with the aid of the following equation:

$$\sigma = \frac{L}{SR} \quad (1)$$

where L is the sample thickness and S is the electrode area in the sample surface.

2.3. Single cell fabrication and electrical performance measurements

The NiO and BCY–GDC with a weight ratio of 6:4 was used for the anode material of single cells, while the cathode was made of $La_{0.8}Sr_{0.4}Co_{0.2}Fe_{0.8}O_{3-\delta}$ (LSCF) and BCY–GDC with a weight ratio of 7:3. A certain amount of the anode powder mixture was loaded into a pressing die with a diameter of 12 mm and then was pressed slightly. Subsequently, the 0.02 g electrolyte powder (BCY–GDC) was added to the surface of the anode disc, and the anode|electrolyte assembly was then pressed with a pressure of 300 MPa to form discs. The anode|electrolyte discs were then sintered at either 1450 °C or 1550 °C for 5 h with a heating rate of 3 °C min^{-1}. The sintered anode|electrolyte half cells (NiO–BCY–GDC|BCY–GDC) were then coated with the LSCF–BCY–GDC cathode using the screen printing process. The sandwich-structure containing NiO–BCY–GDC|BCY–GDC|LSCF–BCY–GDC was sintered at 900 °C for 3 h to form single cells.

The cell performance was measured with a DC electronic load (ITech Electronics model IT8511). Humidified hydrogen (~3% H_2O) was fed to the anode chamber at a flow rate of 25 mL min^{-1}, while the cathode was exposed to atmospheric air. The impedance measurement of the button cells was conducted under open circuit conditions using an impedance apparatus (WAYNE KERR6540A) with the humidified hydrogen (3% H_2O) at the anode and atmospheric air at the cathode. The frequency for the impedance analysis was from 0.1 Hz to 100 kHz with temperatures ranging from 450 to 700 °C.

3. Results and discussion

3.1. Characterization of BCY–GDC composite powders

Fig. 1 shows the X-ray diffraction (XRD) patterns of the BCY, GDC and BCY–GDC powders calcined at 1000 °C. It is found that the BCY sample contains only diffraction peaks of the perovskite structure (PDF 82-2372), and only diffraction peaks corresponding to fluorite structure (PDF 75-0161) are present in GDC. Furthermore, the peaks of the composite electrolyte powders are just the superposition of the peaks of the perovskite structure BCY and fluorite structure GDC with no any other phases. This indicates that the BCY–GDC composite electrolyte powder is the mixture of BCY and GDC. According to the peak broadening of the XRD patterns and the Scherre formula, the average crystallite sizes of BCY and GDC in the composite powder are 24 nm and 38 nm, respectively. Therefore, nanometer BCY–GDC double-matrix-composite electrolyte powders can be obtained via a one-step citric acid–nitrate gel combustion method.

3.2. Properties of sintered electrolytes

Fig. 2 shows the XRD patterns of BCY–GDC pellets sintered at different temperatures. The diffraction pattern clearly shows the

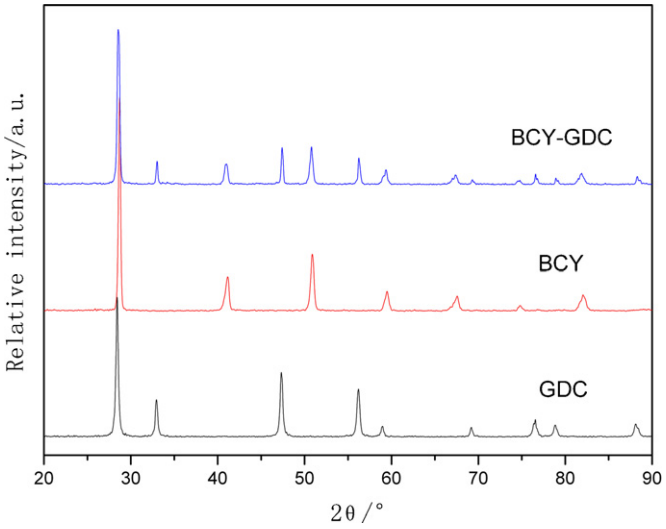

Fig. 1. X-ray diffraction (XRD) patterns of the BCY, GDC and BCY–GDC powders.

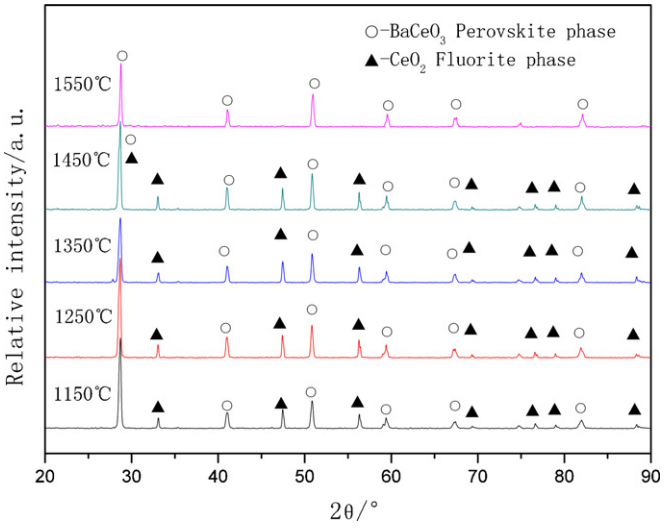

Fig. 2. XRD patterns of BCY–GDC pellets sintered at different temperatures.

superposition of BCY and GDC phases for the composite electrolytes sintered at the temperature range 1150–1450 °C, indicating no new phase formation during sintering at this temperature range. However, it is noted that the peaks of GDC disappear completely in the XRD pattern of the composite electrolyte sintered at 1550 °C. Only a perovskite phase is present after sintering at 1500 °C, suggesting that the BCY–GDC double-matrix-composite electrolyte has changed into a single phase, i.e., a new phase has formed via the reaction between BCY and GDC.

Table 1 summarizes the lattice constants and the unit cell volume of each phase in various samples. Literature values [20,21] and PDF card values are also included for comparison. It is found that the unit cell volume of the GDC in the composite electrolyte sintered at different temperatures is between that of CeO_2 and $Ce_{0.9}Gd_{0.1}O_{1.95}$, which means that the mole content of Gd in the GDC is in the range of 0–10%. In other words, the GDC in the composite electrolyte is $Ce_{0.9+x}Gd_{0.1-x}O_{2-\delta}$. For the perovskite structure the crystal cell volume of the perovskite structure is found to be smaller than that of $BaCe_{0.8}Y_{0.2}O_{3-\alpha}$. Since the crystal cell volume of $BaCeO_3$ decreases with the addition of Y and Gd (see Table 1), it is safe to conclude that some Ce in the BCY has been substituted by Gd. Therefore, the BCY in the composite electrolyte is $BaCe_{0.8-x}Y_{0.2}Gd_xO_{3-\alpha}$.

The most interesting phenomenon of this study is the disappearance of the CeO_2-based fluorite structure when the composite electrolyte is sintered at 1550 °C. It is known that the melting point of CeO_2 is about 2700 °C [22], which is much higher than the sintering temperature (1550 °C). Furthermore, CeO_2-based fluorite structures such as CeO_2-doped with Y or Gd are stable at 1550 °C [16,23–25]. Thus, the disappearance of the GDC phase cannot be due to volatilization, and therefore it is concluded that the CeO_2-based fluorite phase has reacted with the $BaCeO_3$-based perovskite phase and transformed into a novel $BaCeO_3$ perovskite phase which contains the elements of Ba, Ce, Y, Gd and O. Based on the composition of the starting materials (BCY + GDC), the composition of the new phase will be $BaCe_{1.6}Gd_{0.2}Y_{0.2}O_{4.9-\alpha}$ (BCGY).

Fig. 3 shows the relative density of BCY–GDC composite electrolyte pellets as a function of the sintering temperature. As expected, the relative densities of composite electrolyte pellets depend strongly on the sintering temperature. The relative density increases from 63% to almost 100% of the theoretical value as the sintering temperature increases from 1150 °C to 1550 °C. Note that the relative density can be higher than 96% at sintering temperature of 1450 °C, which can meet the impermeability demand of SOFC electrolytes. Fig. 4 shows SEM images of the surfaces of composite electrolyte pellets sintered at 1150 °C, 1350 °C, 1450 °C, and 1550 °C for 5 h. It can be seen that the composite electrolyte becomes denser with the increase in the sintering temperature. This trend is in good agreement with the densities determined via Archimedes principle (Fig. 3). Dense electrolyte pellets with a limited number of pores formed at the 1450 °C sintering (Fig. 4c) suggest a good sintering ability of the composite powders. The average grain size of sintered bodies is about 1 μm after sintering at 1450 °C. The average grain

Table 1
Lattice constants and unit cell volume of single phase, composite samples and literature values.

Sample	$BaCeO_3$ perovskite phase				CeO_2 fluorite phase		Reference
	a (Å)	b (Å)	c (Å)	V (Å^3)	a (Å)	V (Å^3)	
BCY–GDC 1150 °C	8.7724	6.235	6.219	340.15	5.4159	158.86	This work
BCY–GDC 1250 °C	8.7737	6.2316	6.2199	340.07	5.4179	159.03	This work
BCY–GDC 1350 °C	8.7813	6.2253	6.2176	339.89	5.4159	158.86	This work
BCY–GDC 1450 °C	8.7697	6.234	6.2157	339.82	5.4149	158.77	This work
BCY–GDC 1550 °C	8.7633	6.232	6.2201	339.7			This work
$Ce_{0.8}Gd_{0.2}O_{1.9}$ (1450 °C)					5.4228	159.47	This work
CeO_2					5.4124	158.55	PDF 81-0792
$Ce_{0.9}Gd_{0.1}O_{1.95}$					5.418	159.04	PDF 75-0161
$Ce_{0.8}Gd_{0.2}O_{1.9}$					5.423	159.5	[20]
$BaCeO_3$	8.7953	6.2622	6.2334	343.33			PDF 85-2155
$BaCe_{0.8}Gd_{0.2}O_{2-\gamma}$	8.816	6.233	6.18	338.8			[21]
$BaCe_{0.85}Gd_{0.15}O_{2-\varepsilon}$	8.86	6.231	6.211	342.9			[21]
$BaCe_{0.8}Y_{0.2}O_{3-\delta}$ (1450 °C)	8.7668	6.24	6.2195	340.2			This work
$BaCe_{0.9}Y_{0.1}O_{2.95}$	8.7704	6.2386	6.2232	340.5			PDF 82-2372

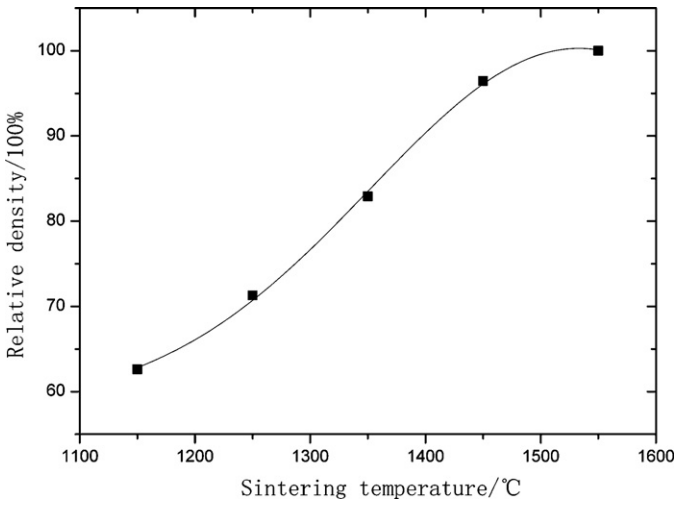

Fig. 3. Relative densities of BCY–GDC composite electrolyte pellets as a function of sintering temperature.

size further increases to about 3 μm as the sintering temperature increases to 1550 °C (Fig. 4d).

The shapes of various crystalline phases are found to depend on the sintering temperature. The single phase BCY is cubic hexahedron (Fig. 5a), while the shape of the single phase GDC is irregular polygon. It can be clearly observed that these two kinds of shapes appear in the composite electrolyte sintered at 1450 °C (Fig. 4c). In contrast, there are only grains with cubic hexahedron in the composite electrolyte sintered at 1550 °C (Fig. 4d). This morphology change is consistent with the XRD analysis, showing that there is only one crystalline phase in the 1550 °C sintered samples. Moreover, BCGY has a perovskite crystal structure and thus exhibits the cubic hexahedron morphology. Therefore, it can be concluded that reaction between the CeO_2-based fluorite phase with the $BaCeO_3$-based perovskite phase has taken place at 1550 °C, leading to the formation of a completely new Y and Gd co-doped $BaCeO_3$-based perovskite phase.

The ionic conductivity is a key property for electrolyte materials of SOFCs. Fig. 6 shows the total conductivities of BCY–GDC electrolytes sintered at different temperatures, measured in wet air (3% H_2O). It can be seen that the total conductivity of the BCY–GDC electrolyte increases with the test temperature studied (550–800 °C). This trend is consistent with the behavior of ionic conductors [1,3,5]. Fig. 6 also exhibits an increase in the total conductivity with the sintering temperature. The increase in conductivity with sintering temperature from 1150 to 1450 °C is attributed to the increase in the grain size (Fig. 4). The increase in the grain size leads to a reduction in the area of grain boundaries, which in turn results in an increase in the conductivity because grain boundaries typically have a higher resistance than the bulk [5,26].

The most exciting phenomenon shown in Fig. 6, however, is the dramatic increase in conductivity exhibited by the BCGY phase formed at 1550 °C. Such a drastic increase cannot be explained by the increase in both the grain size and density. Therefore, we have attributed this drastic increase to the formation of the new $BaCeO_3$-based perovskite phase. For the electrolytes sintered at 1450 °C or lower the total conductivity is the sum of the conductivities of the BCY phase (bulk and grain boundaries), the GDC phase (bulk and

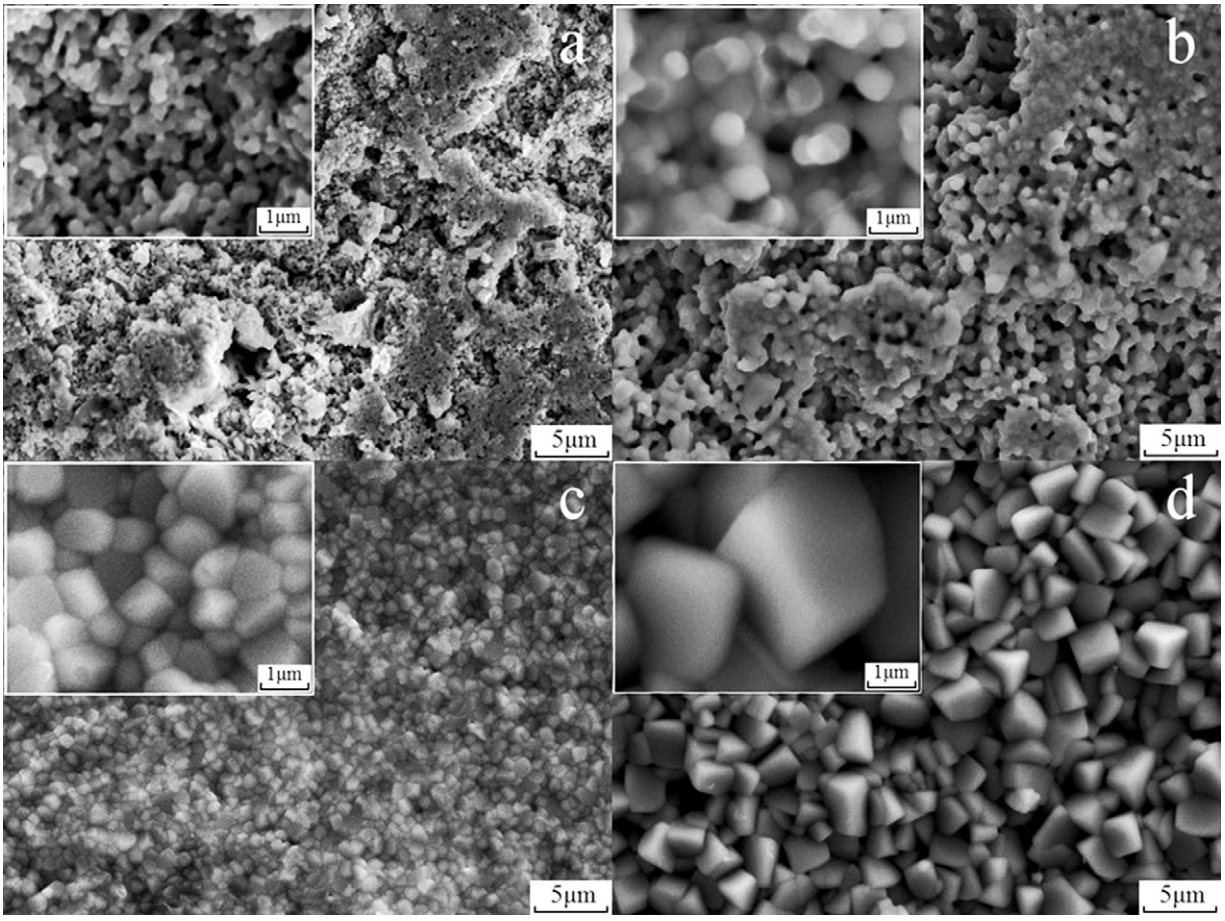

Fig. 4. SEM images of the surfaces of BCY–GDC composite electrolyte pellets sintered at different temperatures: (a) 1150 °C; (b) 1350 °C; (c) 1450 °C; and (d) 1550 °C.

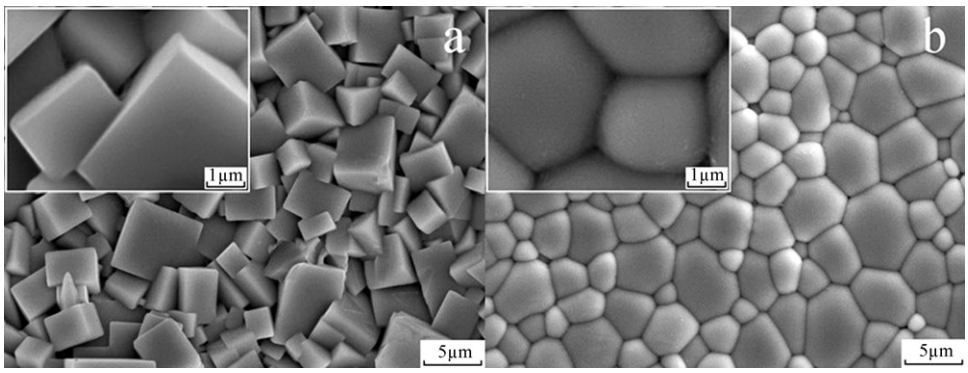

Fig. 5. SEM images of the surfaces of (a) pure BCY and (b) pure GDC pellets sintered at 1550 °C for 5 h.

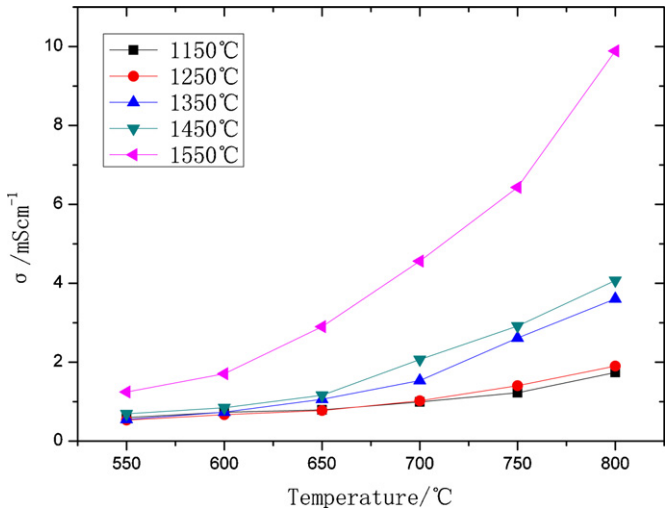

Fig. 6. Total electrical conductivity of BCY–GDC pellets sintered at different temperatures measured under wet air atmosphere (3% H_2O).

grain boundaries) and the BCY–GDC interface. In contrast, the conductivity of the BCGY phase is from the bulk and grain boundaries of the new $BaCeO_3$-based perovskite phase.

Gd-doped barium cerates have been shown to be mixed ionic conductors [21]. BCGY is a Gd and Y co-doped barium cerate. Since Y and Gd have the same valence state, Y is likely to behave like Gd. Thus, the Gd and Y co-doped barium cerate is likely to have the mixed ionic conducting property as Gd-doped barium cerates.

3.3. Impedance analysis of single cells with BCY–GDC electrolytes

In order to assess the electrochemical performance of the fuel cells based on the BCGY electrolyte and the BCY–GDC composite electrolytes, Ni–BCY–GDC anode-supported button cells with a thick BCY–GDC electrolyte membrane (~40 μm) and a LSCF–BCY–GDC cathode were constructed. These button cells will be denoted as Ni–BCY–GDC| BCY–GDC|LSCF–BCY–GDC single cells hereafter. Fig. 7 shows the impedance spectra of such single cells with the BCGY electrolyte. These impedance spectra were measured under open-circuit conditions at different temperatures using electrochemical impedance spectroscopy (EIS). Three

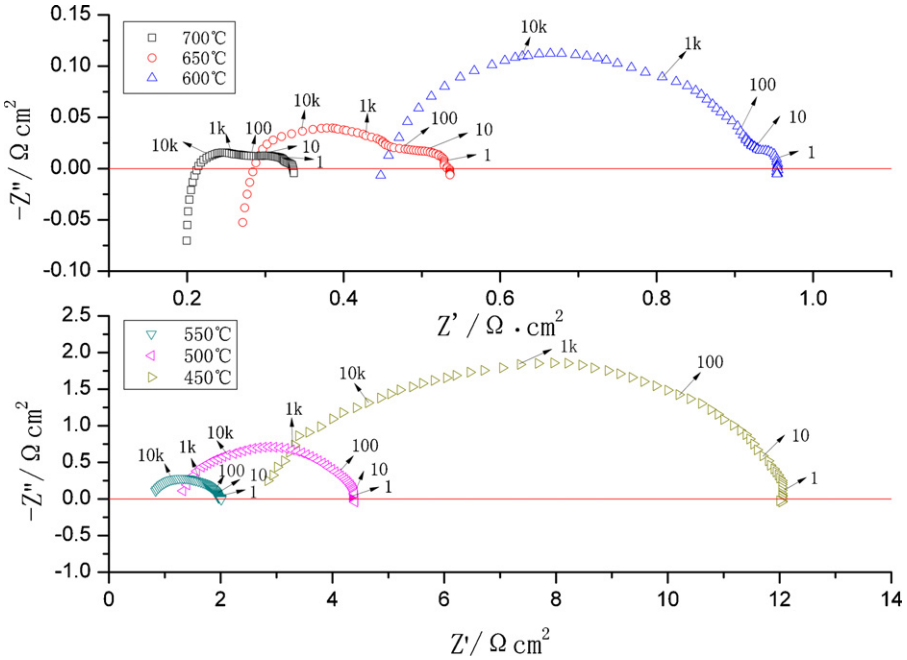

Fig. 7. Impedance spectra of the Ni–BCY–GDC|BCY–GDC (sintered at 1550 °C) |LSCF–BCY–GDC single cells measured under open current conditions at different temperatures. The numbers are the frequencies in hertz.

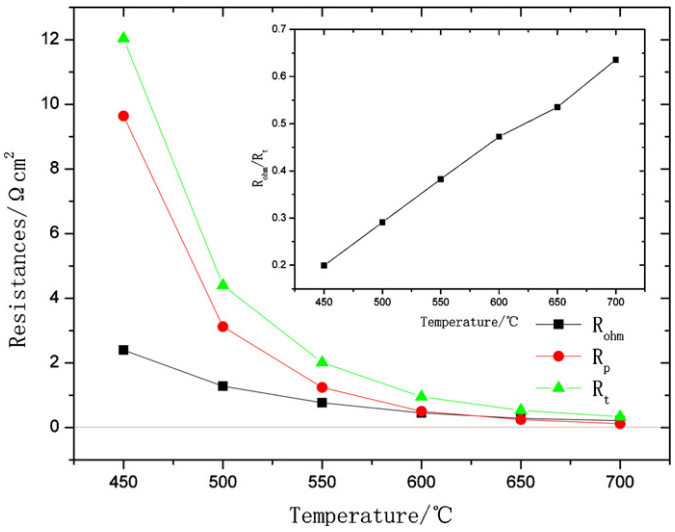

Fig. 8. The cell total resistances (R_t), ohmic resistances (R_{ohm}) and polarization resistances (R_p) of the testing button cell estimated from impedance spectroscopy under open circuit conditions at different temperatures. Inset: the R_{ohm}/R_t ratio at different temperatures.

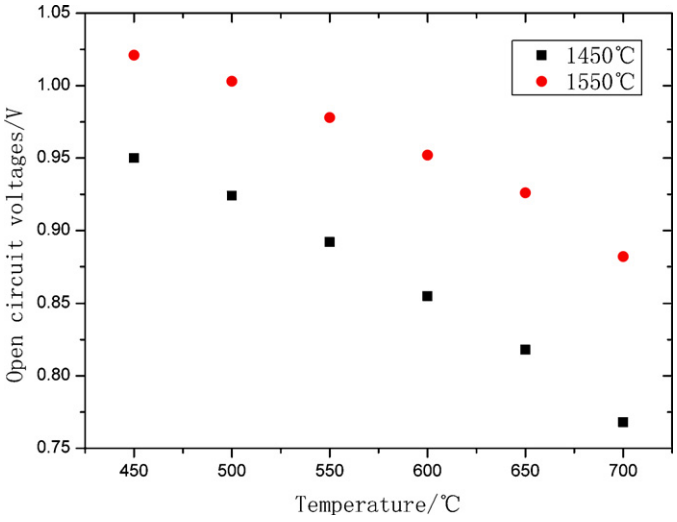

Fig. 9. The OCV of the single cells based on BCY–GDC electrolyte sintered at different temperatures as a function of test temperatures with wet hydrogen (3% H_2O) as the fuel.

parameters can be determined directly from these spectra. The cell total resistance (R_t) is the spectrum interception with the real axis at low frequencies. The interception with the real axis at high frequencies represents the ohmic resistance (R_{ohm}) of the cell, which includes the resistance of the electrolyte, the contact resistance associated with the interface, and the resistances of the electrodes and Ag wires. The difference between the total resistance and the ohmic resistance represents the polarization resistance (R_p) of the cell. The structure of porous composite electrodes significantly affects the active sites for electrochemical reactions (activation polarization), the effective electronic and ionic resistivities (ohmic polarization), and the electrode pore size (concentration polarization). Therefore, the cell polarization is strongly dependent on the structure of electrodes. Fig. 7 indicates clearly that R_t, R_{ohm} and R_p increase with decreasing the testing temperature.

Fig. 8 shows how R_t, R_{ohm} and R_p of the button cells change with the testing temperature. These data are derived from Fig. 7. The R_{ohm}/R_t ratio as a function of temperature is included as the insert in Fig. 8. Note that the R_{ohm}/R_t ratio increases from 0.2 to 0.64 as temperature increases from 450 °C to 700 °C, clearly indicating that R_{ohm} changes from a minor component of the total resistance to a major component as temperature increases. This trend is due to the faster decrease of R_p than that of R_{ohm} as temperature increases. Specifically, R_{ohm} are 2.40, 1.28, 0.77, 0.45, 0.28 and 0.21 Ω cm², while R_p are 9.64, 3.12, 1.24, 0.50, 0.25 and 0.12 Ω cm² at 450 °C, 500 °C, 550 °C, 600 °C, 650 °C and 700 °C, respectively. As a result, R_p is predominant in the total cell resistance below 550 °C, while R_{ohm} is dominant above 600 °C. Thus, at temperatures lower than 600 °C, the performance of the cell will be mainly limited by R_p which needs to be reduced. In contrast, at temperatures higher than 600 °C, the ionic conductivity of the electrolyte is a key factor in improving the cell performance. Similar results were observed in button cells based on other electrolytes [18,27].

3.4. Performance of fuel cells with BCY–GDC electrolytes

Fig. 9 compares the open circuit voltages (OCV) of single cells with the composite electrolyte sintered at 1450 and 1550 °C, measured with wet H_2 (3% H_2O) as the fuel and static air as the oxidant. The OCV for both cells decreases with increasing temperature. This trend is consistent with the reduced cell potential when temperature increases, as predicted from the Nernst equation [28]. However, the single cells with the electrolyte sintered at 1450 °C have a lower OCV and a faster decrease in the OCV with increasing temperature than the single cells with the electrolyte sintered at 1550 °C. Specifically, the OCV of the cells with the electrolyte sintered at 1550 °C is 1.02 V at 450 °C, whereas the corresponding value for the cells with the electrolyte sintered at 1450 °C is only 0.95 V, i.e., 0.07 V lower than the cells with the electrolyte sintered at 1550 °C. The difference becomes larger (0.11 V) as temperature increases to 700 °C. The low OCV and fast OCV decrease for the electrolyte sintered at 1450 °C are most likely due to the presence of GDC which is a mixed ionic and electronic conductor [1,29,30]. Thus, the BCGY phase not only has a higher electrical conductivity, but also has a lower electronic conductivity, if any, than GDC.

Shown in Fig. 10 are the *I–V* and power density curves of single cells with the BCY–GDC electrolyte sintered at 1450 °C, as a function of the operation temperature tested using wet H_2 as the fuel and static air as the oxidant. The corresponding curves for single cells with the electrolyte sintered at 1550 °C are shown in Fig. 11. It can be seen that the peak power densities of the single cells with the electrolyte sintered at 1450 °C are lower than that of the single cells with the electrolyte sintered at 1550 °C. Specifically, the peak

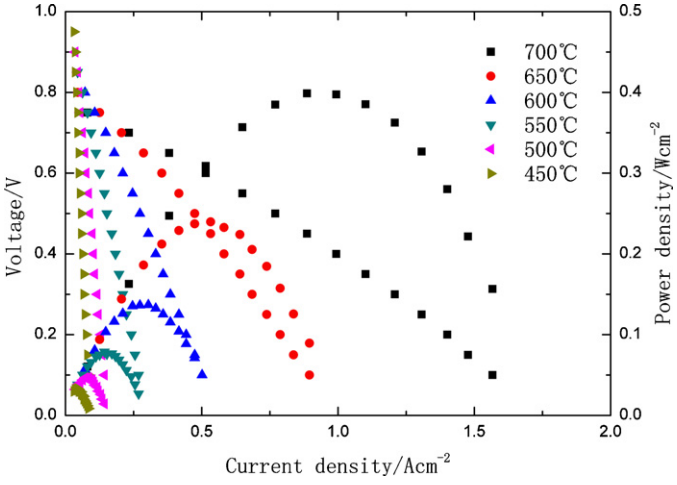

Fig. 10. Current density–voltage and power density curves of the Ni–BCY–GDC|BCY–GDC (sintered at 1450 °C) |LSCF–BCY–GDC single cells tested at different temperatures.

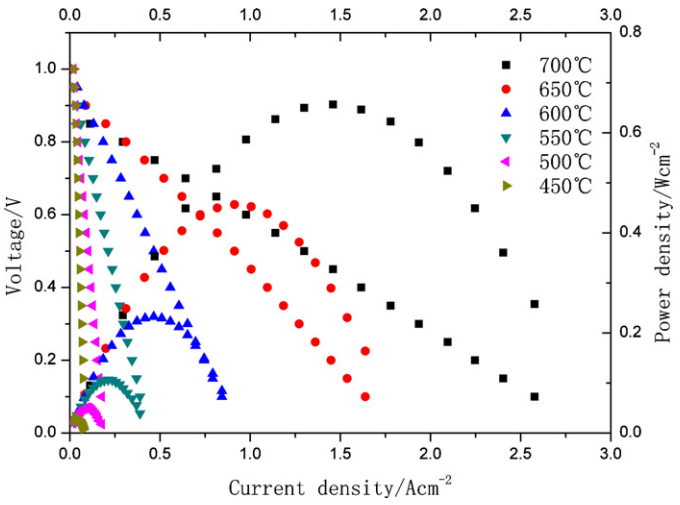

Fig. 11. Current density–voltage and power density curves of the Ni–BCY–GDC|BCY–GDC (sintered at 1550 °C) |LSCF–BCY–GDC single cells tested at different temperatures.

power density of the cells with the electrolyte sintered at 1450 °C is only 0.399 W cm^{-2} at 700 °C, whereas the corresponding value of the cells with the electrolyte sintered at 1550 °C is 0.657 W cm^{-2}, representing ~65% increase over the cells with the electrolyte sintered at 1450 °C. This improvement can be attributed to two major factors. First, the BCGY electrolyte formed at 1550 °C has a higher electrical conductivity than the composite electrolyte sintered at 1450 °C (Fig. 6) because the BCGY electrolyte formed at 1550 °C has a larger grain size, denser membrane and higher intrinsic conductivity than the composite electrolyte sintered at 1450 °C. Second, the BCGY electrolyte has a higher OCV (Fig. 9) because of its lower electronic conductivity than GDC.

Fig. 12 summarizes the peak power densities for all single cells with the electrolyte sintered at either 1450 or 1550 °C. Note that at operation temperatures below 550 °C the peak power densities for all cells are similar, whereas at operation temperatures above 550 °C the peak power densities of the cells with the electrolyte sintered at 1550 °C are higher than that of the cells with the electrolyte sintered at 1450 °C. As explained above, the better performance of the cells with electrolyte sintered at 1550 °C at the high operation

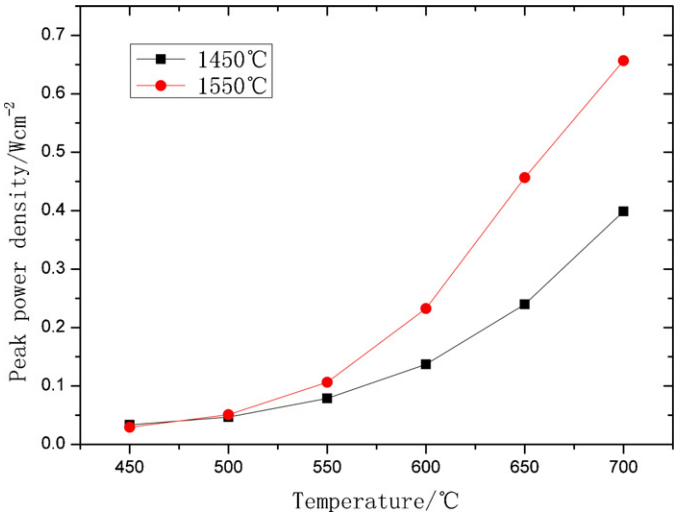

Fig. 12. The peak power density of the single cells with the BCY–GDC electrolyte sintered at different temperatures as a function of test temperatures with wet hydrogen (3% H_2O) as the fuel.

temperature region (600–700 °C) is due to the higher OCV and electrical conductivity derived from the BCGY electrolyte. Note that at the low operation temperature region (450–500 °C) the advantage of a higher OCV (Fig. 9) and electrical conductivity (Fig. 6) derived from the BCGY electrolyte is still present. However, at the low operation temperature region the cell total resistance is dominated by the polarization resistances of the anode and cathode (Fig. 8). Since the single cells with the electrolyte sintered at 1450 and 1550 °C in this study have the similar composition and structure for their anodes and cathodes, they thus have the similar polarization resistance and therefore exhibit the similar peak power densities. This analysis indicates that the electrochemical performance of the cells with the BCGY electrolyte can be enhanced if the anode and cathode are optimized in the future. Finally, it is worthy of mentioning that the electrical output of the cells with the BCGY electrolyte in this work is higher than that of many button cells based on other electrolytes at the same operating temperature [31–34].

4. Conclusions

$BaCe_{0.8}Y_{0.2}O_{3-\delta}$–$Ce_{0.8}Gd_{0.2}O_{1.9}$ (BCY–GDC) composite electrolyte powders (BCY–GDC with a molar ratio 1:1) have been successfully synthesized via a one-step citric acid–nitrate gel combustion method. BCY–GDC composite electrolytes sintered between 1150 °C and 1450 °C are composed of the mixture of BCY and GDC. However, when sintered at 1550 °C BCY and GDC react to form $BaCe_{1.6}Gd_{0.2}Y_{0.2}O_{4.9-\alpha}$ (BCGY) with a perovskite structure. The conductivity of the electrolyte pellets based on the BCGY is higher than that of BCY + GDC composite electrolyte pellets sintered at 1150 °C to 1450 °C. The conductivity of the BCGY phase in wet air (3% H_2O) reaches as high as 0.01 S cm^{-1} at 800 °C.

Single cells constructed using the BCGY electrolyte exhibit higher open circuit voltages than single cells using the composite electrolyte sintered at 1450 °C. Similarly, the cells derived from the BCGY electrolyte have better electrochemical performance than the counterparts constructed using the composite electrolyte sintered at 1450 °C. The peak power density reached by the cells using the BCGY electrolyte is 0.657 W cm^{-2} at 700 °C, showing ~65% increase over the cells with the composite electrolyte sintered at 1450 °C. AC impedance spectroscopy reveals that the total cell resistance of the cells made from the BCGY electrolyte is dominated by the polarization resistance at temperatures below 600 °C, suggesting that the polarization resistances of the cathode and anode need to be improved. However, at temperatures above 600 °C, the total cell resistance is mainly due to the ohmic resistance, which can be reduced by decreasing the thickness of the electrolyte from the present 40 μm to less than 10 μm in the future.

References

[1] B.C.H. Steele, Solid State Ionics 129 (2000) 95–110.
[2] J.S. Ahn, S. Omar, H. Yoon, J.C. Nino, E.D. Wachsman, J. Power Sources 195 (2010) 2131–2135.
[3] C. Xia, M. Liu, Solid State Ionics 152–153 (2002) 423–430.
[4] B. Dalslet, P. Blennow, P. Hendriksen, N. Bonanos, D. Lybye, M. Mogensen, J. Solid State Electrochem. 10 (2006) 547–561.
[5] X. Guo, W. Sigle, J. Maier, J. Am. Ceram. Soc. 86 (2003) 77–87.
[6] C. Guizard, A. Julbe, O. Robbe, S. Sarrade, Catal. Today 104 (2005) 120–125.
[7] H. Inaba, H. Tagawa, Solid State Ionics 83 (1996) 1–16.
[8] E.C. Subbarao, H.S. Maiti, Solid State Ionics 11 (1984) 317–338.
[9] K. Eguchi, T. Setoguchi, T. Inoue, H. Arai, Solid State Ionics 52 (1992) 165–172.
[10] J.M. Im, H.J. You, Y.S. Yoon, D.W. Shin, Ceram. Int. 34 (2008) 877–881.
[11] B.C.H. Steele, K.M. Hori, S. Uchino, Solid State Ionics 135 (2000) 445–450.
[12] T. Tsai, E. Perry, S. Barnett, J. Electrochem. Soc. 144 (1997) 130–132.
[13] T. Inoue, T. Setoguchi, K. Eguchi, H. Arai, Solid State Ionics 35 (1989) 285–291.
[14] Y. Mishima, H. Mitsuyasu, M. Ohtaki, K. Eguchi, J. Electrochem. Soc. 145 (1998) 1004–1007.
[15] M. Khandelwal, A. Venkatasubramanian, T.R.S. Prasanna, P. Gopalan, J. Eur. Ceram. Soc. 31 (2011) 559–568.

[16] A. Venkatasubramanian, P. Gopalan, T.R.S. Prasanna, Int. J. Hydrogen Energy 35 (2010) 4597–4605.
[17] B. Zhu, X. Liu, T. Schober, Electrochem. Commun. 6 (2004) 378–383.
[18] W. Sun, Y. Jiang, Y. Wang, S. Fang, Z. Zhu, W. Liu, J. Power Sources 196 (2011) 62–68.
[19] H.P. Klug, L.E. Alexander, X-ray Diffraction Procedures for Polycrystalline and Amorphous Materials, John Wiley & Sons, Inc., London, 1954.
[20] S.J. Hong, A.V. Virkar, J. Am. Ceram. Soc. 78 (1995) 433–439.
[21] N. Taniguchi, K. Hatoh, J. Niikura, T. Gamo, H. Iwahara, Solid State Ionics 53–56 (Part 2) (1992) 998–1003.
[22] J.-G. Li, T. Ikegami, T. Mori, Acta Mater. 52 (2004) 2221–2228.
[23] L. Gao, M. Zhou, Y. Zheng, H. Gu, H. Chen, L. Guo, J. Power Sources 195 (2010) 3130–3134.
[24] V. Gil, J. Tartaj, C. Moure, P. Duran, Ceram. Int. 33 (2007) 471–475.
[25] T. Ishida, F. Iguchi, K. Sato, T. Hashida, H. Yugami, Solid State Ionics 176 (2005) 2417–2421.
[26] X.-Z. Fu, J.-L. Luo, A.R. Sanger, N. Luo, K.T. Chuang, J. Power Sources 195 (2010) 2659–2663.
[27] W. Sun, Z. Shi, S. Fang, L. Yan, Z. Zhu, W. Liu, Int. J. Hydrogen Energy 35 (2010) 7925–7929.
[28] R.T. Leah, N.P. Brandon, P. Aguiar, J. Power Sources 145 (2005) 336–352.
[29] S. Zha, W. Rauch, M. Liu, Solid State Ionics 166 (2004) 241–250.
[30] J. Liu, B.D. Madsen, Z. Ji, S.A. Barnett, Electrochem. Solid-State Lett. 5 (2002) A122–A124.
[31] M. Matsuda, T. Hosomi, K. Murata, T. Fukui, M. Miyake, Electrochem. Solid-State Lett. 8 (2005) A8–A11.
[32] Z. Tao, Z. Zhu, H. Wang, W. Liu, J. Power Sources 195 (2010) 3481–3484.
[33] C. Hwang, C.-H. Tsai, C.-H. Lo, C.-H. Sun, J. Power Sources 180 (2008) 132–142.
[34] Z. Tao, L. Bi, S. Fang, W. Liu, J. Power Sources 196 (2011) 5840–5843.